



tion, TEM studies, and neutron scattering studies<sup>18–20</sup> give values from 318–328 °C for compositions of about 37–40 % Zn. (Assessing the coherent phase boundary via aging at low temperatures and reheating to find the reversion temperature is problematic due to the complex precipitation kinetics at low temperatures.<sup>7</sup>) Decomposition of the solid solution at temperatures below the coherent phase boundary gives rise to a series of coherent fcc precipitate shapes. The precipitation sequence involves spherical Guinier-Preston (GP) zones,<sup>7,21</sup> coherent ellipsoidal precipitates, and partially coherent platelets [with coherency along (111)].<sup>22–26</sup>

The decomposition of Al-rich  $\text{Al}_x\text{Cu}_{1-x}$  solid solutions also produces coherent GP zones. In fact, Al-Cu alloys provide the textbook example of the formation of GP zones in supersaturated solid solutions.<sup>27,28,21</sup> The specifics of the precipitation sequence are somewhat controversial, but it is generally agreed that coherent platelets of Cu form along (100) directions.<sup>28</sup> Two types of GP zones have been reported, the so-called GP1 and GP2 zones.<sup>28</sup> There have been many measurements of the coherent phase boundaries for GP1 and GP2 zones (see Ref. 75, and references therein) which show a maximum temperature of roughly 200 °C at the solubility limit of 2% Cu. Recently, the mixed-space cluster expansion technique used here has been applied to Al-Cu alloys and the resulting coherent phase boundaries and precipitates predicted.<sup>29</sup> This theoretical approach was shown to provide predictions for the coherent precipitate shapes of GP1 and GP2, and also provides an explanation for the GP1-GP2 transition observed in terms of a size-dependent transition of the equilibrium precipitate shape.

Here, we construct a mixed-space cluster expansion for Al-Zn alloys using first-principles total energy calculations. Then, we compare the resulting phase stability of Al-Zn with the previous calculations of Al-Cu (Ref. 29) in terms of their zero-temperature superlattice energies and ground states, as well as thermodynamic properties such as mixing enthalpies, coherent phase boundaries, and short-range order in the solid solutions. We show how the instability of fcc-Zn is, to a large extent, responsible for many of the thermodynamic properties of Al-Zn, and is hence responsible for the contrast between many properties of Al-Zn and Al-Cu. All of these results are compared with experimental observations, where available. The calculations described here create a basis for a detailed theoretical study of precipitation in Al-Zn.

## II. INSTABILITY OF ELEMENTAL FCC ZN

The constituents of the two considered alloys Cu, Al, and Zn, have different structural preferences: while Cu and Al crystallize in an fcc lattice, Zn is hcp. Confronted with the problem of describing the fcc solid solution in the  $\text{Al}_x\text{Zn}_{1-x}$  alloy system we have to inquire about the stability and elastic properties of this unusual phase: fcc-Zn. Figure 1 compares LDA-calculated total energies of volume-conserving distortions along the three principal crystallographic

many times before.<sup>31-35</sup> However, the most common example is fcc-stable elements (e.g., Cu) which are unstable in the bcc structure, or vice versa. [The 100-type distortion connects the fcc and bcc structures via the Bain path, and the instability of bcc Cu can be seen from the 100 distortion in

where  $a_p(x)$  is the lattice constant that minimizes  $\Delta E_{CS}^{\text{eq}}$  at each  $x$ . Figure 3 presents the constituent strain energy for  $\text{Al}_x\text{Cu}_{1-x}$  and  $\text{Al}_x\text{Zn}_{1-x}$  as function of the Al composition for different directions.<sup>41</sup> We see that (i) all strain energies are about an order of magnitude smaller for Al-Zn than for Al-Cu. In fact, the strain energy in  $\text{Al}_x\text{Zn}_{1-x}$  does not exceed a value of 5 meV/atom for any direction. (ii) The strain energies of the  $\text{Al}_x\text{Zn}_{1-x}$  alloy are characterized by the existence of an elastically soft (111) direction and an elastically hard (100) direction. In contrast, for  $\text{Al}_x\text{Cu}_{1-x}$  the (111) direction is the hardest up to  $x=0.70$ , while (100) is the elastically softest direction between 25 to 100 % Al. The different directional strain behavior of  $\text{Al}_x\text{Zn}_{1-x}$  and  $\text{Al}_x\text{Cu}_{1-x}$  alloys can be illustrated by a three-dimensional parametriza-



TABLE II. Cluster expansion fit for Al-Cu (see Table I for details).

Average fit error (CE, 41 structures): 8.24 meV  
 Average prediction error (0 predictions): —  
 Maximum error: 41.84 meV

| Stoich.                             | $x_{Al}$ | Direction |           |           |                         |       | others                              | others         |
|-------------------------------------|----------|-----------|-----------|-----------|-------------------------|-------|-------------------------------------|----------------|
|                                     |          | (100)     | (110)     | (111)     | (201)                   | (311) |                                     |                |
| <i>Cu</i>                           | 0.0      |           |           |           |                         |       | <i>fcc</i>                          |                |
| direct:                             |          |           |           |           |                         |       | 0.0                                 |                |
| CE:                                 |          |           |           |           |                         |       | -4.4                                |                |
| <i>AlCu<sub>8</sub></i>             | 0.111    |           |           |           |                         |       | <i>Ni<sub>8</sub>Nb<sub>6</sub></i> |                |
|                                     |          |           |           |           |                         |       | -90.8                               |                |
|                                     |          |           |           |           |                         |       | -106.3                              |                |
| <i>AlCu<sub>7</sub></i>             | 0.125    |           |           |           |                         |       | <i>D7<sub>6</sub></i>               |                |
|                                     |          |           |           |           |                         |       | -93.1                               |                |
|                                     |          |           |           |           |                         |       | -108.7                              |                |
| <i>AlCu<sub>3</sub></i>             | 0.25     | <i>Z3</i> | <i>Y3</i> | <i>V3</i> | <i>D0<sub>22b</sub></i> |       | <i>L1<sub>2</sub></i>               | <i>SQS14b*</i> |
|                                     |          | -148.2    | -143.0    | -29.6     | -201.7                  |       | -193.7                              | -118.9         |
|                                     |          | -133.3    | -164.6    | -51.6     | -223.3                  |       | -169.3                              | -129.1         |
| <i>Al<sub>2</sub>Cu<sub>8</sub></i> | 0.25     |           |           |           |                         |       | <i>LPS3b*</i>                       | <i>D023</i>    |
|                                     |          |           |           |           |                         |       | -196.8                              | -199.3         |
|                                     |          |           |           |           |                         |       | -191.9                              | -200.2         |
| <i>Al<sub>3</sub>Cu<sub>9</sub></i> | 0.25     |           |           |           |                         |       | <i>LPS21b</i>                       |                |
|                                     |          |           |           |           |                         |       | -199.7                              |                |
|                                     |          |           |           |           |                         |       | -206.5                              |                |
| <i>AlCu<sub>2</sub></i>             | 0.333    | <i>β2</i> | <i>γ2</i> | <i>α2</i> |                         |       |                                     |                |
|                                     |          | 277.5     | 215.8     | 50.4      |                         |       |                                     |                |

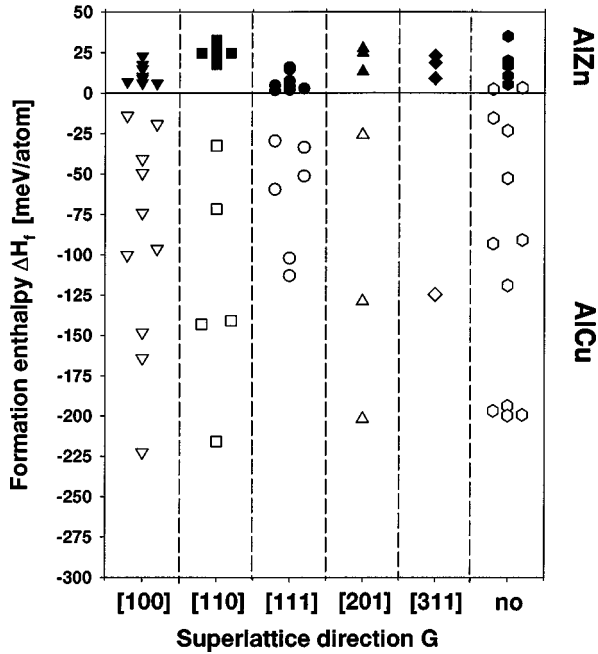


FIG. 5. Fully relaxed LDA formation enthalpies  $\Delta H_f$  for all considered  $\text{Al}_p\text{Zn}_q$  and  $\text{Al}_p\text{Cu}_q$  ordered compounds sorted by superlattice direction. While the  $\text{Al}_p\text{Zn}_q$  compounds have exclusively positive formation enthalpies, the  $\text{Al}_p\text{Cu}_q$  compounds possess nearly all negative formation enthalpies.

layers of Zn]. The calculated  $\Delta H_f$  are given in Tables I and II and plotted in Fig. 5. We note the following:

(i) While for  $\text{Al}_p\text{Cu}_q$  compounds nearly all formation enthalpies are negative, they are exclusively positive for  $\text{Al}_p\text{Zn}_q$ . This already characterizes Al-Cu as ordering system, and Al-Zn as phase separating system. The formation enthalpies of  $\text{Al}_p\text{Cu}_q$  compounds range between

–222.5 meV/atom to +3.2 meV/atom, while for  $\text{Al}_p\text{Zn}_q$  they range only between +1.8 meV/atom to +35.1 meV/atom.

(ii) Formation enthalpies for  $\text{Al}_p\text{Zn}_q$  compounds with layer ordering along the (111) direction are smallest. This is evident in Fig. 6 which shows all directly calculated formation enthalpies of  $\text{Al}_p\text{Zn}_q$  compounds and can be interpreted as a consequence of the unusually low constituent strain energy.

(iii) The formation enthalpies of Al-Zn (110) superlattices are relatively large, even larger than along the (100) superlattices, although Al-Zn also appears to be very soft along (110) (see Fig. 3).

To understand the trends in formation enthalpies we will use the following rough (and admittedly, nonunique) decomposition: We describe the formation enthalpy of any structure as the sum of the constituent strain energy of Eq. (2) and the relaxed “chemical energy” including all other contributions,

$$\Delta H_f(x, \sigma) = \Delta E_{CS}^{\text{eq}}(\sigma) + \Delta E_{\text{chem}}(x, \sigma). \quad (4)$$

The partitioning of Eq. (4) leads to the conclusion that for  $\text{Al}_p\text{Zn}_q$  compounds  $\Delta E_{\text{chem}}$  on the average must be more positive for structures ordered along (110) than (111). Taking into account all directly calculated formation enthalpies of ordered compounds along (111) and (110) into account we get average values of  $\Delta E_{\text{chem}}(111) = 6.6$  meV/atom and  $\Delta E_{\text{chem}}(110) = 24.5$  meV/atom. The averages of the constituent strain energy for considered superlattices amount to  $\Delta E_{CS}^{\text{eq}}(\sigma)(111) = 1.1$  meV/atom and  $\Delta E_{CS}^{\text{eq}}(\sigma)(110) = 1.6$  meV/atom. In other words, for “(111) compounds” even the very soft strain energy gives a fractionally larger contribution to the formation enthalpies shown in Fig. 6, while the fractional contribution of strain to formation enthalpies along (110) is relatively small.

#### D. A detour: The need to use geometrically equivalent $k$ points in evaluating formation enthalpies

The small formation enthalpies in  $\text{Al}_p\text{Zn}_q$  demand extremely careful convergence. In addition to convergence with respect to the basis set, one needs to assure convergence with respect to  $k$  points. Considering Eq. (3), we see that one needs to converge the  $k$  representation for a compound  $A_pB_q$  as well as for the elemental constituents  $A$  and  $B$ . The standard way of accomplishing this is to increase the number of  $k$  points in all 3 systems until convergence is obtained. This can be done using any method of Brillouin zone sampling, e.g., Chadi-Cohen<sup>49</sup> or Monkhorst-Pack.<sup>50</sup> The disadvantage of this approach is that it requires *absolute*  $k$  point convergence for  $A$ ,  $B$  and separately, for  $A_pB_q$ . An alternative method is to take advantage of *relative*  $k$  point convergence.<sup>51</sup>

The idea is to sample the Brillouin zone *equivalently* for  $A$ ,  $B$  and for  $A_pB_q$ . This could be done by considering  $A_pA_q$ ,  $B_pB_q$ , and  $A_pB_q$  as isostructural solids and sample the Brillouin zone of all equally. Then, any relative  $k$ -point sampling error cancels out. This is called the *method of equivalent  $k$  points*.<sup>51</sup> In practice, we do not have to calculate the total energies of  $A_pA_q$  and  $B_pB_q$ , but we can calculate instead the energies of  $A$  and  $B$ , at suitably folded-in  $k$  points.



FIG. 6. Fully relaxed LDA formation enthalpies  $\Delta H_f$  for  $\text{Al}_p\text{Zn}_q$  compounds: The smallest values are found for compounds which are superlattices along the (111) direction.

For comparison three epitaxial energies as well as three formation enthalpies were calculated using  $N \times N \times N$  regular (Monkhorst-Pack) and equivalent  $k$  points for  $N=8,10,12$ . Here,  $N \times N \times N$  is the number of  $k$  points in the first Brillouin-zone before reduction by symmetry. The chosen epitaxial systems are Zn(100) and Zn (111) relaxed at  $a = 7.50$  a.u. ( $a_{\text{eq}}=7.23$  a.u.) as well as Al(110) relaxed at  $a = 7.33$  a.u. ( $a_{\text{eq}}=7.50$  a.u.). The three ordered compounds are  $L1_2$ , which does not allow any cell-vector distortions, as well as  $L1_0$  and  $L1_1$  allowing distortions along the  $c$ -axes in the (100) and (111) directions, respectively. The results are shown in Table III: It can be seen that the  $\Delta H_f$  values for equivalent sets converge much faster than using regular sets. Indeed, even a  $10 \times 10 \times 10$  regular mesh  $k$ -point set for most cases (except  $L1_2$ ) is not sufficient. For equivalent  $k$ -points a set of  $10 \times 10 \times 10$   $k$  points represents the smallest acceptable choice especially for distortions along (111).

To determine the minimum number of equivalent  $k$  points needed we calculate  $\Delta H_f$  for superlattices along (111) direction. The reason for selecting this ordering direction is that atomic movements along (111) are very large due to the unusual epitaxial softness along this direction. These tests (Table IV) show that sometimes even  $12 \times 12 \times 12$  equivalent  $k$  points are not sufficient for convergence: While for the  $L1_2$ ,  $L1_1$ , and  $V2$  structures, the use of  $8 \times 8 \times 8$   $k$  points already leads to stable results, for the  $\alpha 2$ ,  $V3$ ,  $V6$ , and  $V8$  structures this is definitely not the case. For example,  $\Delta H_f$  for  $\alpha 2$  and  $V6$  are  $-4.1$  and  $-9.9$  meV/atom using  $12$

$\times 12 \times 12$  while using  $18 \times 18 \times 18$  gives  $+2.0$  and  $+2.8$  meV/atom, respectively. As a result, a  $12 \times 12 \times 12$  set of  $k$  points would erroneously predict the Al-Zn system to be ordering-type along (111), but phase separating along all other directions. This  $k$ -point problem is connected to unusual small formation enthalpies of  $\text{Al}_x\text{Zn}_{1-x}$ . It should be mentioned that the problem described only appears for compounds with equivalent superlattices along (111), i.e., for compounds showing large cell-vector distortions and atomic movements. Formation enthalpies calculated for other compounds do not show such a high sensitivity to the number of  $k$  points.

#### IV. THERMODYNAMIC QUANTITIES

To calculate finite temperature, thermodynamic properties with first principles accuracy, pair- and multibody effective cluster interactions are needed as input for Monte Carlo simulations. These interactions are generated by use of a mixed-space cluster expansion with directly calculated LDA strain energies and formation enthalpies as input. We next describe the construction of the cluster expansion for Al-Cu and Al-Zn.

##### A. The mixed space cluster expansion for Al-Zn and Al-Cu

It has been demonstrated<sup>42-44,29</sup> that a *mixed-space cluster expansion*<sup>16,17</sup>





for the fcc solid solution relative to fcc constituents, i.e., the fcc-hcp energy difference for Zn was already subtracted. Our calculated first-principles mixing enthalpy  $\Delta H_{\text{AlZn}}(x, 643 \text{ K})$  and the phenomenological fit to experiment of an Mey<sup>53</sup> are compared in Fig. 8(a). The two curves agree very well: Both show a maximum around 40% Zn with a corresponding mixing enthalpy of about 20 meV/atom. A comparison to individual experimental studies of the fcc phase appears to be very difficult, because their results differ profoundly: For example, while calorimetric studies of Wittig and Schöffl<sup>55</sup> ( $T=643 \text{ K}$ ) and Connel and Downie<sup>56</sup> ( $T=637 \text{ K}$ ) lead to a maximum in the enthalpy of mixing at about 25% Zn, electromagnetic field studies by Hilliard, Averbach, and Cohen<sup>57</sup> ( $T=653 \text{ K}$ ) find a maximum around 60% Zn. To our knowledge these discrepancies for the thermodynamic properties of the fcc solid solution are not yet clarified; hence, future experimental studies would be desirable.

We also have calculated the mixing enthalpy of the configurationally-random alloy: Monte Carlo simulations were performed for extremely high temperatures (e.g.,  $T=50\,000 \text{ K}$ ) where almost all atomic exchanges of the Metropolis algorithm are accepted. This simulation samples the configuration space in an unbiased manner, and gives the

energy of the configurationally-random state. The composition dependence of  $\Delta H(\text{random})$  is given in the lower part of Fig. 8. The difference between the results of Fig. 8(a) and those in Fig. 8(b) are due to the energetic effect of short-range order in the solid solution. For the phase separating alloy system  $\text{Al}_x\text{Zn}_{1-x}$  all values are positive exhibiting a maximum around 40% Zn, while for the ordering system  $\text{Al}_x\text{Cu}_{1-x}$  all values are negative exhibiting a minimum around 30% Cu. The mixing enthalpy of the  $\text{Al}_x\text{Zn}_{1-x}$  random alloy at the maximum amounts to +24 meV/atom, while the mixing enthalpy of the  $\text{Al}_x\text{Cu}_{1-x}$  random alloy at the minimum amounts to -130 meV/atom. These calculated enthalpies (without the effects of short-range order) may be compared with measured values<sup>58,59</sup> for disordered Cu-rich alloys which are also shown in Fig. 8. As can be seen, the agreement is very good, especially, if we consider that the theoretical values are for the fully random alloy and a discussion of the cited experimental investigations by Hultgren<sup>13</sup> gives an error estimate of  $\pm 30 \text{ meV/atom}$  for these measured values.

The limited solubility of Cu in Al means that it is not possible to compare the entire curve in Fig. 8 with experiment, but rather only the Al-rich dilute limit. The dilute heat of solution for Cu in Al is computed for the atom cluster expansion approach: The calculated value for an  $\text{Al}_{0.99}\text{Cu}_{0.01}$  alloy is  $\Delta H_{\text{solution}} = -50 \text{ meV/Cu atom}$  for the random alloy, and  $\Delta H_{\text{solution}}(T=700 \text{ K}) = -70 \text{ meV/Cu atom}$  when short-range order is taken into account. Both of these values are extremely small (in magnitude) compared to the formation enthalpies of ordered Al-rich compounds, e.g.,  $\Delta H(\text{Z1}) = -96.2 \text{ meV/atom} = -385 \text{ meV/Cu atom}$ , nearly an order of magnitude larger than the heat of solution. The smallness of the heat of solution is due to the asymmetric shape of the random alloy energy in Fig. 8. The curvature of the random alloy energy changes sign and the mixing energy nearly becomes positive for Al-rich alloys. Interestingly, this





One might be surprised by the clustering tendency of the solid solution since almost all the calculated formation enthalpies for ordered compounds (Table II) and mixing energies of random alloys (

## APPENDIX: PSEUDOPOTENTIAL AND LAPW METHODS

The full-potential linearized augmented plane-wave method (LAPW) (Ref. 64) was applied to calculate formation enthalpies for  $Al_pCu_q$  compounds, while a plane-wave code for pseudopotentials (PP) was applied to calculate first principles total energies for  $Al_pZn_q$ . In both approaches the exchange correlation term was always treated by the local density approximation of Ceperley and Alder<sup>65</sup> in the parametrization of Perdew and Zunger.<sup>66</sup>

In the *plane-wave pseudopotential calculation*, the kinetic energy and the implementation of Kleinman-Bylander<sup>67</sup> non-local potentials are performed in reciprocal space, the local potential and exchange correlation energy are calculated in real space. For a given occupied screened potential, the occupied eigenstates at different  $k$  points are calculated using the conjugate gradient method. The conjugate gradient line minimization is performed one state at a time. Since the input potential is fixed during the conjugate gradient process, analytic energy curves can be used to determine the energy minimum in the line minimization. At any given time, only the wave functions of one  $k$  point need to be stored in the memory, while all other wave functions are stored on disk. This method allows calculations with a large number of  $k$  points as required in our study. As in the conventional approach,<sup>68</sup> an outside loop is provided to converge the self-consistent field. While Kerker's approach<sup>73</sup> is used to mix the input and output screened potential differently at different reciprocal vector components, Pulay's algorithm<sup>74</sup> is used to take advantage of all the previous input-output potential pairs to determine the optimal input potential for the next iteration.

The atomic pseudopotentials (PP) were generated using the scheme of Troullier and Martins<sup>69</sup> whereby 3d electrons of Cu and Zn were treated as valence electrons. The cutoff radii used for  $s$ ,  $p$ , and  $d$  pseudopotentials are  $r_s(Al) = 2.2 \text{ \AA}$ ,  $r_p(Al) = 2.0 \text{ \AA}$ ,  $r_s(Cu) = 1.8 \text{ \AA}$ ,  $r_p(Cu) = 2.3 \text{ \AA}$ ,  $r_d(Cu) = 1.5 \text{ \AA}$ ,  $r_s(Zn) = 2.0 \text{ \AA}$ ,  $r_p(Zn) = 2.6 \text{ \AA}$ ,  $r_d(Zn) = 2.0 \text{ \AA}$ . Atomic PP and all-electron eigenvalues agree for all elements better than 0.07 meV. To guarantee stability of the PP a number of transferability tests

- <sup>12</sup>B. Schoenfeld, H. Reolofs, A. Malik, G. Kostorz, J. Plessing, and H. Neuhauser, *Acta Mater.* **44**, 335 (1996).
- <sup>13</sup>R. Hultgren, P. D. Desai, D. T. Hawkins, M. Gleiser, and K. K. Kelley, *Selected Values of the Thermodynamic Properties of Binary Alloys* (American Society for Metals, Metals Park, Ohio, 1973).
- <sup>14</sup>M. Hansen, *Constitution of Binary Alloys* (McGraw-Hill, New York, 1958).
- <sup>15</sup>T. B. Massalski,